

See discussions, stats, and author profiles for this publication at: <https://www.researchgate.net/publication/252261619>

Characterizing bio-optical and ecological features of algal bloom waters for detection and tracking from space

ARTICLE *in* PROCEEDINGS OF SPIE - THE INTERNATIONAL SOCIETY FOR OPTICAL ENGINEERING · APRIL 2010

Impact Factor: 0.2 · DOI: 10.1117/12.852444

READS

24

8 AUTHORS, INCLUDING:



[Irina Gladkova](#)

City College of New York

58 PUBLICATIONS 170 CITATIONS

[SEE PROFILE](#)



[Michael D. Grossberg](#)

City College of New York

87 PUBLICATIONS 2,100 CITATIONS

[SEE PROFILE](#)



[Soe Hlaing](#)

City College of New York

29 PUBLICATIONS 177 CITATIONS

[SEE PROFILE](#)

Characterizing bio-optical and ecological features of algal bloom waters for detection and tracking from space

S. Ahmed, R Amin, I. Gladkova, A. Gilerson, M. Grossberg,

S. Hlaing, F. Shahriar, P. Alabi.

Optical Remote Sensing Laboratory

The City College of New York, 160 Convent Avenue, New York, NY 10031

ABSTRACT

The detection and monitoring of harmful algal blooms using in-situ field measurements is both labor intensive and is practically limited on achievable temporal and spatial resolutions, since field measurements are typically carried out at a series of discrete points and at discrete times, with practical limitations on temporal continuity. The planning and preparation of remedial measures to reduce health risks, etc., requires detection approaches which can effectively cover larger areas with contiguous spatial resolutions, and at the same time offer a more comprehensive and contemporaneous snapshot of entire blooms as they occur. This is beyond capabilities of in-situ measurements and it is in this context that satellite Ocean Color sensors offer potential advantages for bloom detection and monitoring. In this paper we examine the applications and limitations of an approach we have recently developed for the detection of *K. brevis* blooms from satellite Ocean Color Sensors measurements, the Red Band Difference Technique, and compare it to other detection algorithm approaches, including a new statistical based approach also proposed here. To achieve more uniform standards of comparisons, the performance of different techniques for detection are applied to the same specific verified blooms occurring off the West Florida Shelf (WFS) that have been verified by in-situ measurements.

Keywords: Ocean optics, remote sensing, ocean color, harmful algal bloom, red tide, MODIS.

1. INTRODUCTION

The detection and monitoring of harmful algal blooms using in-situ field measurements is both labor intensive and is practically limited on achievable temporal and spatial resolutions, since field measurements are typically carried out at a series of discrete points and at discrete times, with practical limitations on temporal continuity. The planning and preparation of remedial measures to reduce health risks, etc., requires detection approaches which can effectively cover larger areas with contiguous spatial resolutions, and at the same time offer a more comprehensive and contemporaneous snapshot of entire blooms as they occur. This is beyond capabilities of in-situ measurements and it is in this context that satellite Ocean Color sensors offer potential advantages for bloom detection and monitoring.

It is worthwhile to first consider the features of *K. brevis* blooms and their special optical characteristics which impact their detection from satellite Ocean Color observations. The toxic dinoflagellate *Karenia brevis* (*K. brevis*) formerly named *Gymnodinium breve* [1] is the most common of the more than 40 species of toxic microalgae that live in the Gulf of Mexico. Blooms of *K. brevis* have been observed throughout the Gulf of Mexico. Most frequently they occur along the WFS. A nearly annual event, they are usually observed between late fall and early spring. *K. brevis* blooms have many negative impacts due to brevetoxin. This associated toxin causes death in fish, birds, and marine mammals [2]. It also can irritate human eyes and respiratory systems once it becomes airborne in sea spray [3, 4].

The optical characteristics of *K. brevis* have been extensively studied [5-12]. It was observed by Cannizaro et al., (2008) [5] that *K. brevis* blooms typically exhibit lower backscattering compared to other phytoplankton and that this low backscattering efficiency was related to its large size (20-40 μm) and low index of refraction (~ 1.05) [6]. Since backscattered light in ocean waters is typically dominated by that from submicron particles [13, 14], this would also suggest that the low backscatter associated with *K. brevis* blooms may also reflect lower associated concentration of submicron particles [15, 16]. It was further suggested by Schofield et al., (2006) [8] that the toxicity of *K. brevis* cells

may also contribute to the lower concentration of non-algal particles by directly inhibiting bacterial growth and/or altering the organic material available for heterotrophic consumption.

These characteristics of *K. brevis* impact different satellite detection approaches. The most effective means in operational use is that proposed by Stumpf et al., (2003) [17] using the magnitude of the difference between satellite chlorophyll concentration estimates and a background mean of chlorophyll estimates for the previous 0.5-2.5 months as an index for detecting bloom areas. At NOAA NESDIS CoastWatch, this method is now used operationally to alert for possible blooms in West Florida. Cannizzaro et al., (2008) [5] proposed another technique based on in situ data that uses the backscattering/chlorophyll ratio to discriminate between *K. brevis* and other blooms. They determined that *K. brevis* has lower backscatter characteristics than blooms of other diatoms and dinoflagellate species. Both of these methods are based on using the blue-green region of the spectrum. Unfortunately, blue-green reflectance ratio algorithms [18-20] have been found to perform poorly in coastal waters due to increased absorption of colored dissolved organic matter (CDOM), increased particle scattering, inaccurate atmospheric corrections and shallow bottom reflectance. Hu et al., (2005) [21] used Fluorescence Line Height (FLH) to detect and monitor *K. brevis* bloom on the WFS. However, our studies have shown that FLH, conventionally used, strongly overestimates the chlorophyll fluorescence signal under high elastic scattering conditions, resulting in false positives [22-24].

In this paper we examine the applications and limitations of the Red Band Difference (RBD) technique and a related selective *K. brevis* bloom classification index (KBBI) recently reported by us for bloom detection and classification of *K. brevis* blooms in the WFS from satellite Ocean Color Sensors measurements [25], and compare it to other detection algorithm approaches, including a new statistically based approach also proposed here. To achieve more uniform standard of comparisons, the performance of different techniques for detection are applied to the same specific blooms occurring off the West Florida Shelf (WFS) that have been verified by in-situ measurements. While this may limit the generality of the conclusions, we believe it helps reduce ambiguities and highlight some important common criteria impacting efficacies of different approaches. For these illustrations, data is used from both the Moderate Resolution Imaging Spectroradiometer (MODIS) ocean color sensor which has several bands in the red and near-infrared (NIR) regions and the Medium Resolution Imaging Spectrometer (MERIS) sensor.

In Section 2 that follows, the procedures for obtaining satellite imagery are briefly described. In Section 3, we briefly review the background of the RBD technique, present simulations of remote-sensing reflectance spectra ($R_{rs}(\lambda)$) for *K. brevis* and non-*K. brevis* blooms, review RBD detection and classification techniques and discuss their backgrounds. Section 4 applies these techniques to satellite ocean color data and shows examples of detection, tracing, and classification of *K. brevis* blooms. We also compare the RBD detection and FLH techniques, and discuss possible modifications of processing procedures to FLH to improve *K. brevis* bloom detection, and carry out an analysis of the impacts of atmospheric correction algorithms on the RBD and KBBI techniques. Section 5 discusses a statistically based approach for the detection of *K. brevis* bloom and examines its application in the WFS and compares its results to RBD. Section 6 summarizes the results of the comparison of different bloom detection techniques.

2. SATELLITE DATA AND IMAGE PROCESSING

MODIS imagery of WFS was obtained for different *K. brevis* blooms recorded in the literature dating from 2001 to 2006 from the NASA Ocean Color Website [26] and processed to obtain the normalized water-leaving radiance ($nLw(\lambda)$) for visible and NIR bands, and FLH using SeaDAS version 6.0. The top of the atmosphere signals were corrected for the atmosphere using the standard NIR [27] method. The data was processed with a pixel size of 1km equal to the nominal pixel size of the sensor's ocean color bands.

3. RBD TECHNIQUE

3.1 Background of RBD Detection and KBBI Classification Algorithms

The essence of our approach is that the water-leaving radiance spectra of *K. brevis* and non-*K. brevis* blooms have distinctive features in the red region of the spectrum which can be used to detect and classify *K. brevis* blooms. The red

spectral region is particularly attractive since it is less contaminated by CDOM and bottom reflectance, and is less susceptible to atmospheric correction difficulties than the blue-green region. As a consequence, uncertainties in bloom detection algorithms are reduced if this spectral region is used instead of the blue-green region. The distinguishing optical features of *K. brevis* and non-*K. brevis* blooms are demonstrated in Fig. 1, obtained from simulations of reflectance, and described in [25]. The simulated elastic reflectance $R_{rs}(\lambda)$, without chlorophyll fluorescence (green spectra) shows a trough around 675nm due to the absorption of chlorophyll for both types of blooms. When a fluorescence signal is included in the simulation (red spectra), the trough of the *K. brevis* bloom shifts toward shorter wavelengths around 667nm, or less, depending on chlorophyll concentrations and its quantum yield while the trough of non-*K. brevis* bloom remains around 675nm. The shift in the *K. brevis* spectra is due to the fact that *K. brevis* exhibit lower backscattering efficiency, so the fluorescence signal dominates the red reflectance spectral region. Because of the overlap of the phytoplankton absorption and chlorophyll fluorescence emission, when fluorescence is a significant portion of the reflectance signal, the trough in the red region shifts towards shorter wavelengths, which is the case for *K. brevis*. On the other hand, non-*K. brevis* blooms (mostly dominated by diatoms) have higher backscattering efficiency, so reflection is dominated by the elastic backscattering component, and therefore the fluorescence signal represents a smaller portion of the total reflectance, and is too weak a contributor (compared to the backscatter signal) to result in any significant overall impact on the spectral distribution in that range. As a consequence, the trough of non-*K. brevis* blooms reflectance remains around the maximum of the phytoplankton absorption spectra (Fig. 1).

3.2 Detection Algorithm

Based on the above observations showing that the minimum of $R_{rs}(\lambda)$ can shift from the phytoplankton absorption maximum, around 678nm, to shorter wavelengths, around 667nm, with significant chlorophyll fluorescence contributions in the red spectral region, Fig. 1, we can define a bloom detection technique which we identify simply as the Red Band Difference (RBD) as follows:

$$RBD = nLw(678) - nLw(667)$$

Simulation shows that the positive RBD values ($> 1mg / m^3$ of Chlorophyll) are primarily due to the fluorescence signal which correlates strongly with the chlorophyll concentration of the *K. brevis*. Because of this strong correlation, it becomes possible to quantify *K. brevis* and other blooms with similar characteristics in terms of the chlorophyll concentrations more accurately than the standard reflectance band ratio algorithms [18-20] by developing some empirical relationship between the RBD and the bloom (*K. brevis* and other low backscattering blooms) chlorophyll using in situ data.

Since the RBD technique may also be able to detect blooms of other species, particularly the low backscattering ones, we defined [25], and discuss below, an additional *K. brevis* bloom classification technique, KBBI, to discriminate *K. brevis* blooms from other blooms and bloom like features such as CDOM plumes, sediment plumes and bottom reflectance.

3.3 Classification Algorithm

We defined the *K. brevis* bloom index (KBBI) as follows:

$$KBBI = \frac{nLw(678) - nLw(667)}{nLw(678) + nLw(667)} \quad (2)$$

The KBBI technique is primarily based on the fact that total particulate backscattering associated with *K. brevis* is different from that for non-*K. brevis* blooms. Since *K. brevis* bloom water is known to have lower total particulate backscattering [5- 8] than the non-*K. brevis* bloom waters, the water-leaving radiance signal is much weaker for *K. brevis* blooms than for the non-*K. brevis* blooms since it is largely proportional to backscattering. As a consequence, the denominator of Eq.2, which is just the sum of the two MODIS red bands (band 13 and band 14), becomes much larger for non-*K. brevis* blooms than for *K. brevis* blooms. Furthermore, the numerator of Eq.2, which is the RBD, is much more pronounced for *K. brevis* blooms than the non-*K. brevis* blooms. Therefore, the KBBI values for *K. brevis* are usually higher than that of non-*K. brevis*, thus permitting the separation [25] of the two. In the WFS values of KBBI > 0.3 RBD were found to distinguish *K. brevis* from other blooms [25].

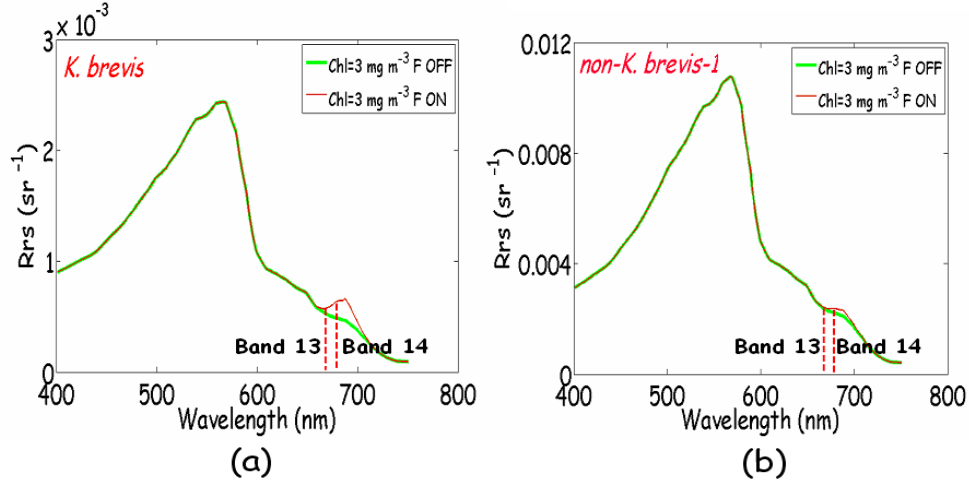


Figure 1. Modeled remote sensing reflectance spectra for *K. brevis* cell concentrations (a) greater than 10^4 cells/l (*K. brevis* bloom) and (b) less than 10^4 cells/l (non-*K. brevis*-1 bloom) for the $Chl = 3 \text{ mg/m}^3$ and $a_{dg}(440) = 0.25 \text{ m}^{-1}$. The solid green spectra are when chlorophyll fluorescence is excluded (“F OFF”) from the simulation and solid red spectra are when fluorescence is included (“F ON”) in the simulation assuming 0.75% quantum yield. Band 13 and 14 are MODIS bands centered at 667nm and 678nm respectively.

4. RESULTS

4.1 Detection of *K. brevis* Blooms

Using the RBD detection technique, we detected various *K. brevis* blooms in the Gulf of Mexico, and reported this in [25]. Figs. 2a and 2b show two examples of *K. brevis* in the WFS detected by RBD and confirmed by in-situ data [21, 30]. The RBD images are created for MODIS (Aqua) images November 13, 2004 and September 21, 2006 [21, 30]. According to [21] the November 13 bloom by mid-late November contained high concentrations ($> 10^5 \text{ cells/l}$) of *K. brevis* cells and caused higher mortalities of fish and dolphins. The bloom drifted southward and expanded to form a large curved patch around 25.5 °N 82.5 °W from early November to mid December, and in subsequent weeks the bloom moved further to the south and formed a continuous band parallel to the Florida Keys [21]. These results are found to match reasonably well with cell count data from in-situ measurements, obtained from [29] which were overlaid on top of the images in Fig 2, with H (black) and L (magenta) representing $> 10^6 \text{ cells/l}$ and $< 10^5 \text{ cells/l}$ respectively. Our analysis, reported in [25] of satellite data coupled with simulated data [25] shows that using a threshold of $\text{RBD} > 0.15 \text{ W/m}^2/\mu\text{m/sr}$ readily identifies legitimate bloom areas. The simulations showed that to reach this RBD threshold value may require chlorophyll as high as 5 mg/m^3 with an assumed 0.75% fluorescence quantum yield. By using a $Chl > 1 \text{ mg/m}^3$ to define a blooming condition [21], the simulation results show that an RBD threshold value lower than $0.15 \text{ W/m}^2/\mu\text{m/sr}$ is possible. However this lower threshold will increase false positives from satellite data analysis. Thus a compromise between simulations and satellite data analysis was made to arrive at the $0.15 \text{ W/m}^2/\mu\text{m/sr}$ RBD threshold. Application of the $\text{KBBI} > 0.3$ RBD as discussed in [25] confirmed the blooms to be *K. brevis*, as shown in Figs 2c and 2d.

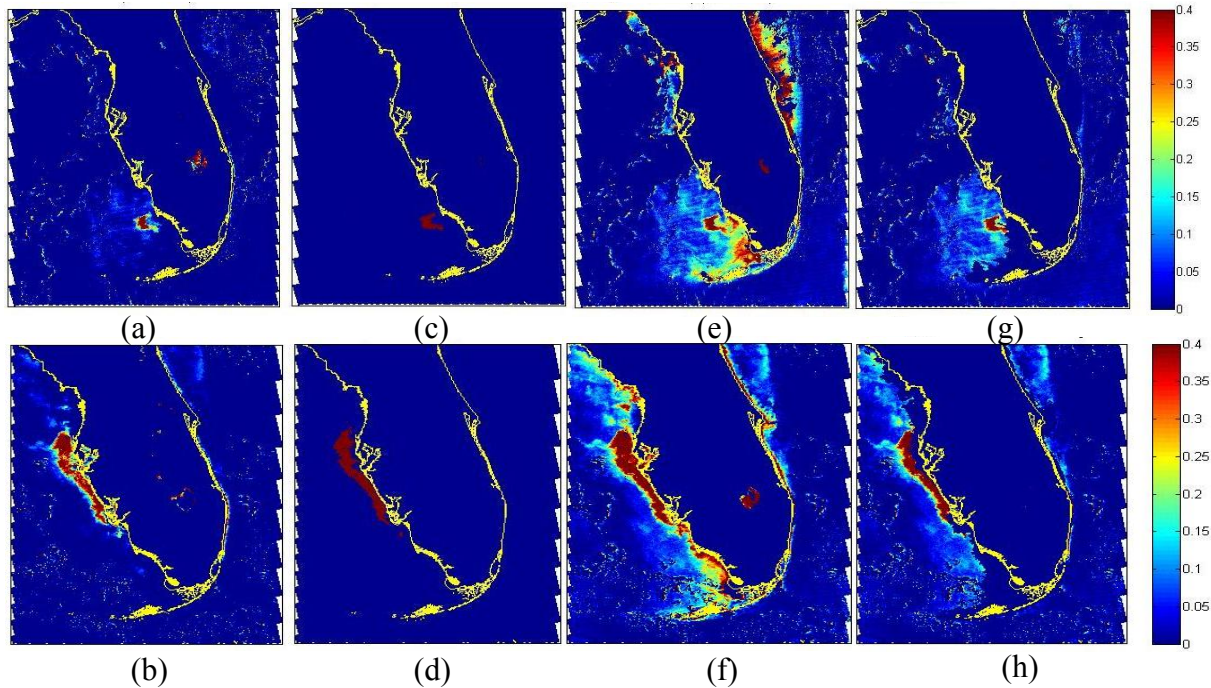


Figure 2. MODIS (Aqua) images of the WFS (a) RBD ($W / m^2 / \mu m / sr$) image of 13 November 2004, (b) RBD ($W / m^2 / \mu m / sr$) of 21 September 2006, (c) KBBI image of 13 November 2004, (d) KBBI image of 21 September 2006, (e) FLH ($W / m^2 / \mu m / sr$) image of 13 November 2004, (f) FLH ($W / m^2 / \mu m / sr$) image of 21 September 2006, (g) FLH ($W / m^2 / \mu m / sr$) image 13 November 2004 filtered for low scattering pixels (h) FLH ($W / m^2 / \mu m / sr$) image 21 September 2006 filtered to eliminate high scattering pixels.

4.2 Comparison between RBD and FLH

Although FLH can sometimes be used to detect blooms [21], it breaks down in highly scattering waters, where high red peak values are primarily due to contributions from elastic scattering modulated by chlorophyll absorption rather than the fluorescence, thus falsely indicating possible blooms. Thus, as the concentration of NAP increases, radiance generally raises as well, and the fluorescence peak becomes a less prominent component of increased total signal.

In contrast, the RBD technique is found to easily differentiate between the two effects, giving positive values in truly bloomed waters and negative values in highly scattering waters. The performance of MODIS FLH calculations can be assessed for turbid waters by comparing FLH values with true fluorescence values at 685nm. Simulations show that the true fluorescence signal at 685 nm decreases as a fraction of the total signal for increasing concentration of NAP. However, MODIS FLH shows an opposite trend and a significant overestimation of the true fluorescence signal. The most dramatic effect is the overestimation of true fluorescence when chlorophyll is low and NAP increases. Similar results were found in [23, 24, 31]. Tomlinson, et al., (2008) [32] also pointed out that FLH was unreliable in the area surrounding the Florida Keys; giving elevated values in all of the images they examined which is in agreement with our analysis of satellite imagery for this region. Clearly, the FLH algorithm can breakdown for turbid waters and if used for *K. brevis* bloom detection would also flag pixels with turbid waters as possible *K. brevis* blooms. On the other hand, the RBD technique only detects true blooms and gives negative or near zero values for highly scattering waters. It is further reinforced by the KBBI classification technique. This is more clearly illustrated in Fig. 3a, which shows the MODIS Aqua FLH bloom image from November 13, 2004 on the WFS, and is in contrast to Fig. 3b which shows equivalent RBD bloom image. To examine whether the intense regions in the FLH image are due to blooms or highly scattering waters, we took three spectra from the three supposedly bloomed regions (bloomed, turbid-1, and turbid-2) as indicated by FLH (Fig. 3a) and plotted the resultant spectra in Fig. 3c. We see that the true *K. brevis* bloom spectrum (Fig. 3b; red) differs significantly from the other two spectra particularly in the blue-green region of the optical spectrum where they both give significantly higher values than the bloomed spectra. So the spectra (Fig. 3c; green and blue) taken from turbid-1 and turbid-2 region of Fig. 3a are due to highly scattering waters, and not characteristic of *K. brevis*. Furthermore, it is seen that the signals in the red bands of these spectra are also significantly different where the *K.*

brevis bloom spectra (Fig. 3c; red) has a positive slope from 667nm band to 678nm band while other two have negative slopes. The slope is negative only when water is highly scattering. Therefore, the region in Fig. 3a indicated by turbid-1 and turbid-2 must be due to highly scattering waters and not *K. brevis* blooms. Those false blooms signals based on FLH clearly disappear in the RBD image (Fig. 3b). since the RBD value is not only below the $0.15 W / m^2 / \mu m / sr$ threshold for *k.brevis* bloom discussed above, but is actually negative, ie there is no bloom detection in these areas.

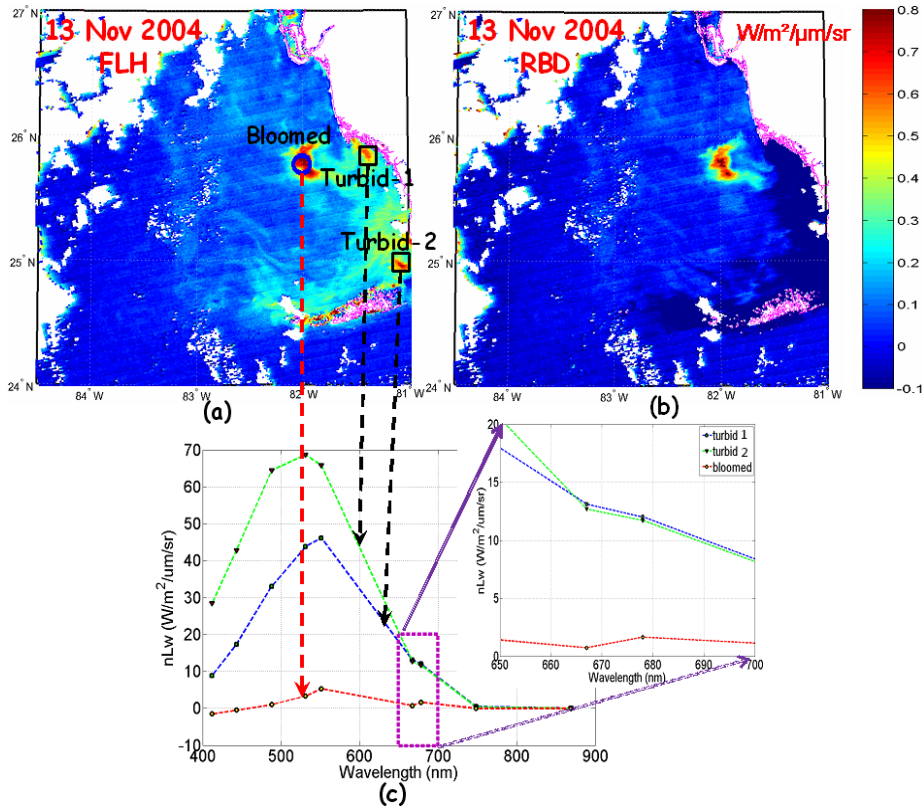


Figure 3. MODIS (Aqua) bloom image from 13 November 2004 for the WFS (a) FLH ($W / m^2 / \mu m / sr$) image, (b) RBD ($W / m^2 / \mu m / sr$) image and (c) Normalized-water leaving radiance spectra taken from the bloomed and turbid waters indicated by “circle” and “squares” respectively in the FLH image.

Since it is the increased scatter encountered in coastal waters that results in false positives when using the FLH technique for *KBrevis* retrievals, it may be possible to achieve similar results using FLH as obtained by using RBD, since the latter essentially uses the fluorescence when the near IR peak legitimately represents the fluorescence signal and is not due to scattering. This can be achieved for the FLH approach if one sets an upper limit on acceptable level of scattering contribution to the FLH peak, using the reflectance at 667 nanometers as a proxy. The impact of this can be seen in Fig 2g, which has an upper limit filter of $1.2 W / m^2 / \mu m / sr$ on the 667 nm band, rejecting FLH for higher values. This reduces the FLH image to one very similar to the equivalent RBD image repeated as Fig 2a, and can be contrasted with the unfiltered FLH image Fig. 2e. In reality, this filtering out of high scatter values is similar to the stricture put on rejecting RBD values below $0.15 W / m^2 / \mu m / sr$ (However, it should be noted that RBD has additionally a self limiting feature, in that higher scattering values at 667 nm give negative values of RBD.). The same approach unfortunately does not work by putting the same stricture on images of chlorophyll in the same region derived using the blue green algorithm, since the latter does not depend on a fluorescence measurement, and is further complicated by overlap of CDOM absorption/fluorescence in coastal waters.

5. STATISTICAL APPROACH - CLASSIFIER FOR KARENIA BREVIS IN WSF

Florida's HAB historical database is one of the largest and longest continually recorded electronic HAB databases in the United States [34]. The historic HAB data is provided by the Fish and Wildlife Research Institute and is available for free download from [35]. This organization provides a detailed GIS point shape file of sampling locations for the phytoplankton that causes *K.brevis*. Sampling site dates range from August 1953 through the latest available spatially verified data. The HAB shape file is a spatial representation of information gathered in the HAB Historical Database, and can be used to construct a classifier aimed at detecting the presence/absence of *K.brevis* from satellite imagery. The database contains over 64,053 records of concentrations of *K.brevis* red tide in Florida waters, from 1954 to 2006. Containing data from over 78 agencies, institutes, universities, and researchers, the database has widely varying numbers of observations, years of collection, spatial or specific areas of collection, and sampling efforts. The variables available for analysis are spatial location, sampling date, collecting agency, depth of collection (for most observations), temperature (for some observations), and either *K.brevis* counts or presence/absence data.

It has been shown [36] that the above data sets are too sparse in both time and space to directly address such questions as the overall WFS status and trends of *K.brevis* at a given time, or understanding of the life cycle of blooms (initiation, development, movement and deterioration). However in [36], some subsets of the data were found to be dense enough in both time and space to permit analysis based on the probability distribution of *K.brevis*. In this section we briefly describe our approach to construct a classifier for absence/presence of *K.brevis*. In this work we used variables from the historic HAB database: location (latitude/longitude), time (day) and the degree to which *K.brevis* was present. Associated with each observation in the data base, there is a satellite product based observational vector. This vector is made up of the following variables: chlorophyll, normalized water leaving radiance at wavelengths 443, 551, and 667, and sea surface temperature, matching the time and location of the HAB database measurement. The HAB measured ground truths together with the corresponding observation vector values are used as training set to train a binary classifier. Once trained, this classifier is used to predict the HAB or no HAB state from the satellite based observation vector alone.

That allowed us to build a training data set for a binary classifier that can relate *K.brevis* presence to satellite observations, and therefore use these to detect blooms. In this process, satellite observations, are tagged according to bloom or no bloom conditions. Each observation has a related 5 dimensional observational vector, obtained as a satellite product, which includes variables such as chlorophyll, normalized water leaving radiances at wavelengths 443, 551, and 667, and sea surface temperature, which can then be used as variables in a training set by matching up location and time from the HAB database, and used to train the classifier.

MODIS flies on board two satellites (Terra and Aqua, launched on December 1999 and May 2002, respectively). In this work we have used gridded Level 3 MODIS data provided by NASA. The data is stored in a representation of a global, equal-area grid cells which have resolution of 4.6 by 4.6km. Level 3 data can be obtained for the NASA's ftp site [37]. We decided to use Aqua satellite in this study since it has fewer overall number of pixels covered by clouds. The overall cloud coverage over the ocean for the period from 2002 to 2009 for both Aqua and Terra is shown in Figure 4. Pixels with smaller values indicate less clouds during the considered period. All pixels corresponding to land have a flagged value 1.

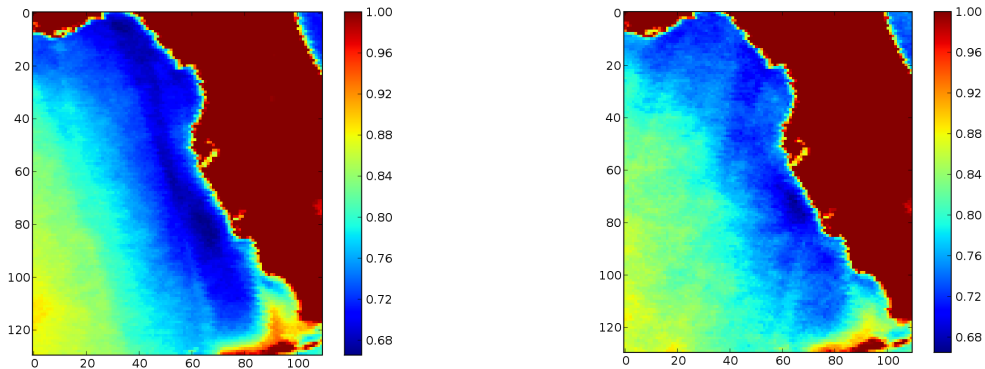


Figure 4. Cloud coverage for Aqua (left) and Terra (right).

Level 3 gridded data includes variables such as chlorophyll, normalized water leaving radiances at wavelengths 443, 551, and 667, and sea surface temperature. Diagram demonstrating the data organization is shown on Figure 5. There are five subdirectories corresponding to each of the five variables. The next level of subdirectories correspond to the years from 2002 to 2009, each of which has 365 (or 366 for leap years) files containing 2 dimensional gridded global product. We can use these variables in our training set by matching up location and time from the HAB database. Dotted path on the Figure 5 shows the process of finding the values that are used in the training data set.

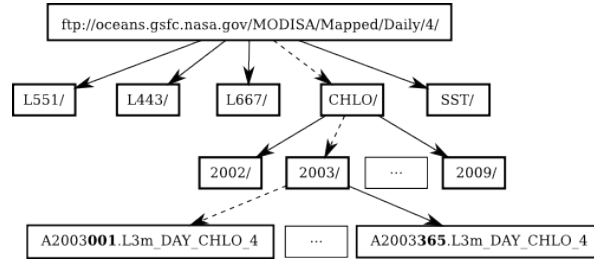


Figure 5. Block-diagram showing Level 3 MODIS data structure. Dotted arrows specify the path of selecting one value for the training data set given the name of the variable, date and location.

The process of creating training data set is shown in Figure 6. First, we filter out entries in the HAB database spatially if they don't fall in the Florida coastal region, and temporally if they are for a date not available in MODIS Ocean Level 3 product. Then the latitudes and longitudes are converted to the rows and columns, and then to file offset. The file offset, date, and variable name uniquely identify a pixel in the Ocean Level 3 dataset, which is read in. The whole image for the whole globe need not be read in because, given the row/column location, we can read individual pixels at an offset in the image, which significantly speeds up the process of creating the training database. Once the data for all the variables is gathered, observations that have been flagged as having cloud or land are filtered out, resulting in the final dataset used for training. If HAB category is "medium" or "high", it is included in the positive case. If it is "not present", it is included in the negative case. Other categories corresponding to less than 100,000 cells/liter were not included in this study. That resulted in 236 positive and 778 negative observations in this training dataset.

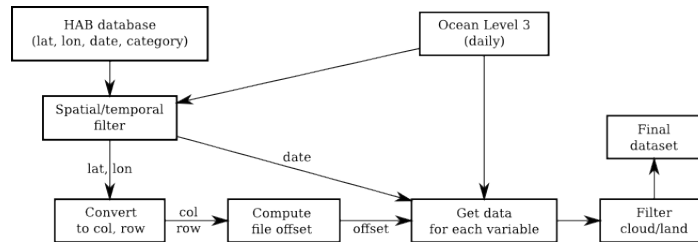


Figure 6. Block-diagram showing steps for obtaining Training Data Set.

The initial dimensionality of the training set is 5, corresponding to five mentioned above variables available in the gridded format. We then decided to use a non-linear procedure known in machine learning as kernel trick. This is a standard method for using a linear classifier algorithm to solve a non-linear problem by mapping the original non-linear observations into a higher-dimensional space, where the linear classifier is subsequently used. This makes a linear classification in the new space equivalent to non-linear classification in the original space. We have used quadratic mapping and a fast algorithm known as the Ho-Kashyap learning rule [38]. The diagram describing procedure for finding the classifier is shown in Figure 7.

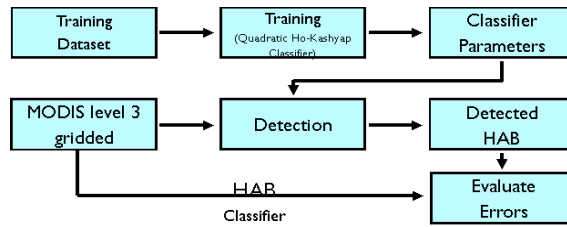
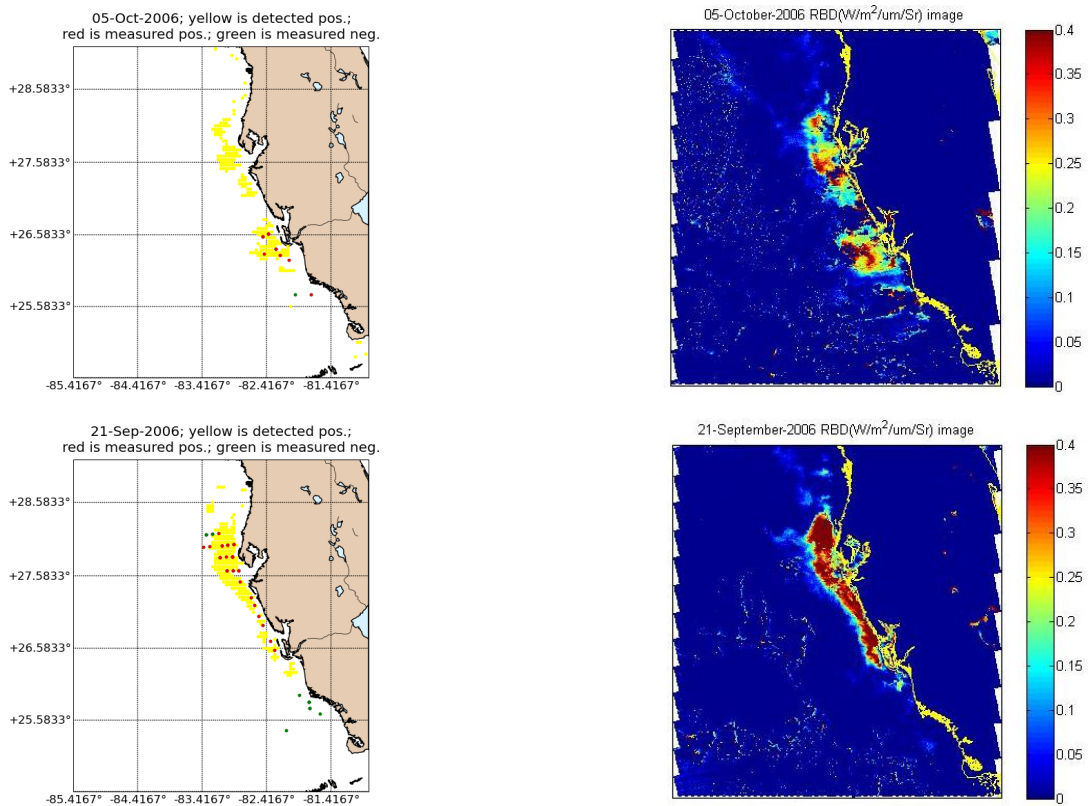


Figure 7. Block-diagram showing showing steps for training the HAB classifier.

Outputs obtained from the classifier described above are shown in the Fig.8. Locations where our algorithm detects presence of *K. brevis* are marked with yellow dots. The red and green dots respectively mark the positive and negative cases as specified in the historical database. The initial results of this approach appear promising. Fig 8 below matches blooms retrieved using this approach, against blooms detected by in-situ measurements covering the same time period, as well as in-situ measurements which showed an absence of blooms.



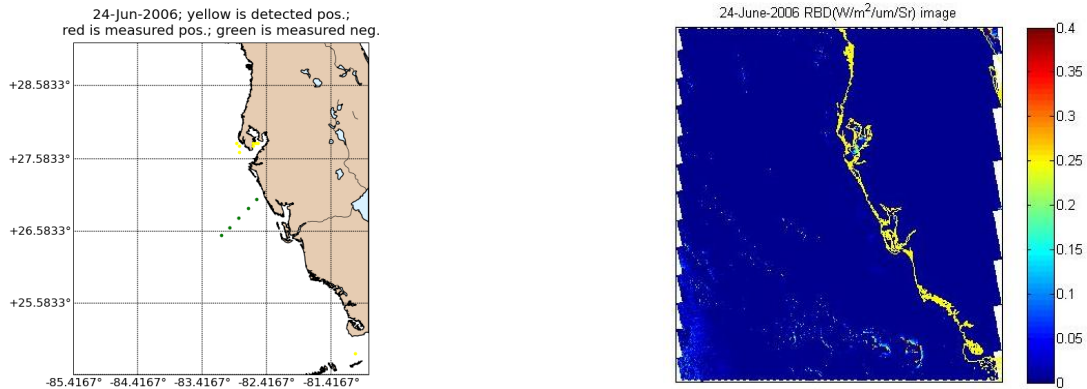


Figure 8. Results of the HAB classifier. Green and red dots correspond to ground truth as given by historical database. Yellow dots correspond to the detected locations of HAB by our classifier. For comparison, an RBD retrieval for 21 September, 2006 is shown adjacent to a statistical retrieval for the same date. There is a good match up between the two.

These results show that there is generally a relatively good match up between blooms retrieved/detected by this technique and blooms measured by in-situ measurements. There are also relatively few, if any false positives, ie where the technique identifies blooms where it is known from in-situ field measurements that none exist. For comparison purposes, Fig 8 also shows RBD retrievals next to a statistical retrievals for the same date, showing good agreement between the two. RBD images selected were based on rejection of any negative values rather than $RBD < 0.15W/m^2/\mu m/sr$. It should be noted that these results represent a true test of the technique since the algal blooms shown in Fig. 8, and detected by the classifier technique as well as their related data were not part of the training sets.

6. Discussion & Conclusions

Chlorophyll retrieval from reflectance spectra remains a challenge in coastal waters, and may even be an impossible task in some cases, particularly when CDOM concentrations are high [33]. MODIS red bands 13 and 14 were designed with high signal-to-noise ratios to avoid various problems including CDOM for retrievals of fluorescence, and hence chlorophyll. However, in highly scattering waters, typical in coastal areas, the fluorescence component represents a only a small portion of the total reflectance peak observed in the red spectral region and it becomes difficult to distinguish the fluorescence component from the elastic component which them dominates the total signal. When low concentrations of NAP and low scattering conditions exist, the peak in the red spectral region becomes chlorophyll fluorescence dominated. Furthermore, this spectral region is less affected by CDOM, shallow bottom, and even atmospheric correction uncertainties than the blue-green region. Since the *K. brevis* bloom is known to have a much lower backscattering efficiency, and to co-exist with generally low scattering waters, the red signals from *K. brevis* blooms are usually largely dominated by the *K. brevis* chlorophyll fluorescence. The RBD technique takes advantage of this fluorescence dominated signal to detect these types of blooms. Normalization then makes it possible for the KBBI technique to discriminate *K. brevis* from non-*K. brevis* blooms. This approach was shown to be quite effective when applied to *K. brevis* bloom conditions in the WFS.

Comparisons with FLH retrievals in the same waters with the same bloom conditions show that in contrast to RBD, many false positives are detected. These are primarily due to increased NAP scattering which enhances the FLH peak in the red spectral region, which is then erroneously correlated with fluorescence. This is in contrast to the RBD/KBBI technique where increased NAP scattering leads to unacceptable small or negative RBD values. This largely eliminates false positives for *K. brevis* detection in typical water conditions obtaining in the WFS bloom regions. It is possible to achieve nearly similar results for FLH as with RBD by applying a filter to FLH measurements. That is by using the 667 nm reflection as a proxy for NAP scattering and filtering out all FLH measurements above a certain threshold value.

A statistical approach, still in its early stages, was tried using a *K. brevis* classifier for WFS waters, and making use of a large existing data base from the The Fish and Wildlife Research Institute [34]. This has extensive data over many years on actual blooms, their intensity and location in WFS. This was dense enough to permit development of probability distributions for the occurrence of *K. Brevis*, which were then correlated with MPDIS measurements from at the 453, 551

and 667 nm bands. The initial results of this approach appear promising. They show relatively good detection of a actual blooms with few false positives, and a good match up with RBD for the same blooms. Both the statistical and RBD approaches warrant continued study, more rigorous testing and extension beyond the WFS region.

REFERENCES

- [1]. <http://www.floridaconservation.org/>
- [2]. J. H. Landsberg, and K. A. Steidinger, "A historical review of *Gymnodium breve* red tides implicated in mass mortalities of the manatee (*Trichechus manatus latirostris*) in Florida, USA," In: Reguera, B., Blanco, J., Fernandez, M.L., Wyatt, T. (Eds.), Proceedings of the 8th International Conference on Harmful Algal Blooms, Vigo, Spain, pp. 97-100, (1998)
- [3]. W. H. Hemmert, "The public health implications of *Gymnodinium breve* red tides, A review of the literature and recent events" In: LoCicero, V.R. (Eds.), Proceedings of the First International Conference on Toxic Dinoflagellate Blooms, pp. 489-497, (1975)
- [4]. S. Asai, J. J. Krzanowski, W. H. Anderson, D. F. Martin, J. B. Polson, R. F. Lockey, S. C. Bukantz, and A. Szentivanyi, "Effects of the toxin of red tide, *Ptychodiscus brevis*, on canine tracheal smooth muscle: a possible new asthma-triggering mechanism," J. Allerg. Clinic. Immunol. **69**, 418-428, (1982)
- [5]. J. P. Cannizzaro, K. L. Carder, F. R. Chen, C. A. Heil, and G. A. Vargo, "A novel technique for detection of the toxic dinoflagellate *Karenia brevis* in the Gulf of Mexico from remotely sensed ocean color data," Continent. Shel. Res. **28**, 137-158, (2008)
- [6]. K. L. Mahoney, "Backscattering of light by *Karenia brevis* and implications for optical detection and monitoring," PhD dissertation, Univ. of South. Miss., Stennis Space Cent. (2003)
- [7]. K. L. Carder, R. G. Steward, "A remote-sensing reflectance model of a red-tide dinoflagellate off west Florida," Limnol. Oceanogr. **30**, 286-298, (1985)
- [8]. O. Schofield, J. Kerfoot, K. Mahoney, M. Moline, M. Oliver, S. Lohrenz, and G. Kirkpatrick, "Vertical migration of the toxic dinoflagellate *Karenia brevis* and the impact on ocean optical properties," J. Geophys. Res., **111**, (2006)
- [9]. G. J. Kirkpatrick, D. F. Millie, M. A. Moline, O. Schofield, "Optical discrimination of a phytoplankton species in natural mixed populations," Limnol. Oceanogr. **45**, 467-4718, (2000)
- [10]. D. F. Millie, G. J. Kirkpatrick, B. T. Vinyard, "Relating photosynthetic pigments and in vivo optical density spectra to irradiance for the Florida red-tide dinoflagellate *Gymnodinium breve*," Marine Ecology Progress Series **120**, 65-75, (1995)
- [11]. D. F. Millie, O. M. Schofield, G. J. Kirkpatrick, G. Johnsen, P. A. Tester, B. T. Vinyard, "Detection of harmful algal blooms using photopigments and absorption signatures: a case study of the Florida red tide dinoflagellate, *Gymnodinium breve*," Limnol. Oceanogr. **42**, 1240-1251, (1997)
- [12]. S. E. Lohrenz, G. L. Fahnenstiel, G. J. Kirkpatrick, C. L. Carroll, K. A. Kelly, "Microphotometric assessment of spectral absorption and its potential application for characterization of harmful algal species," Journal of Phycology **35**, 1438-1446, (1999)
- [13]. A. Morel, and Y. Ahn, "Optics of heterotrophic nanoflagellates and ciliates: A tentative assessment of their scattering role in oceanic waters compared to those of bacteria and algal cells," J. Mar. Res. **49**, 177-202, (1991)
- [14]. D. Stramski, and D. A. Kiefer, "Light scattering in microorganisms in the open ocean," Prog. Oceanogr. **28**, 343-383, (1991)
- [15]. O. Ulloa, S. Sathyendranath, and T. Platt, "Effect of the particle-size distribution on the backscattering ratio in seawater," Appl. Opt. **33**, 7070-7077, (1994)
- [16]. M. S. Twardowski, E. Boss, J. B. Macdonald, W. S. Pegau, A. H. Barnard, and J. R. V. Zaneveld, "A model for estimating bulk refractive index from the optical backscattering ratio and the implications for understanding particle composition in case I and case II waters," J. Geophys. Res. **106**, 14129-14142, (2001)

- [17]. R. P. Stumpf, M. E. Culver, P. A. Tester, M. Tomlinson, G. J. Kirkpatrick, B. A. Pederson, E. Truby, V. Ransibrahmanakul, and M. Soracco, "Monitoring *Karenia brevis* blooms in the Gulf of Mexico using satellite ocean color imagery and other data," *Harmful Algae* **2**, 147-160, (2003)
- [18]. J. E. O'Reilly, S. Maritorena, D. Siegel, M. C. O'Brien, D. Toole, B. G., Mitchell, et al., "Ocean color chlorophyll a algorithms for SeaWiFS, OC2, and OC4: version 4," In: Hooker, S. B. & Firestone, E. R. (Eds.), *SeaWiFS Postlaunch Calibration and Validation Analyses, Part 3 SeaWiFS Postlaunch Technical Report Series*, (pp. 9-23) Greenbelt, Maryland: NASA, Goddard Space Flight Center (2000)
- [19]. H. R. Gordon, D. K. Clark, J. W. Brown, O. B. Brown, R. H. Evans, W. W. Broenkow, "Phytoplankton pigment concentrations in the Middle Atlantic Bight: comparison of ship determinations and CZCS estimates," *Appl. Opt.* **22**, 20-36, (1983)
- [20]. K. L. Carder, F. R. Chen, Z. P. Lee, S. K. Hawes, D. Kamykowski, "Semi-analytic moderate-resolution imaging spectrometer algorithms for chlorophyll a and absorption with bio-optical domains based on nitrate-depletion temperatures," *J. Geophys. Res.* **104**, 5403-5422, (1999)
- [21]. C. Hu, F. E. Muller-Karger, C. Taylor, K. L. Carder, C. Kelble, E. Johns, and C. A. Heil, "Red tide detection and tracing using MODIS fluorescence data: A regional example in SW Florida coastal waters," *Remote Sens. Environ.* **97**, 311-321, (2005)
- [22]. A. Gilerson, J. Zhou, S. Hlaing, I. Ioannou, R. Amin, B. Gross, F. Moshary, and S. Ahmed, "Fluorescence contribution to reflectance spectra for a variety of coastal waters," *Proc. Of SPIE* **6680** (2007)
- [23]. A. Gilerson, J. Zhou, S. Hlaing, I. Ioannou, J. Schalles, B. Gross, F. Moshary, and S. Ahemd, "Fluorescence component in the reflectance spectra from coastal waters. Dependence on water composition," *Opt. Express*, **15**, 15702-15721 (2007)
- [24]. Gilerson, J. Zhou, S. Hlaing, I. Ioannou, B. Gross, F. Moshary, and S. Ahmed, "Fluorescence component in the reflectance spectra from coastal waters. II. Performance of retrieval algorithms," *Opt. Express* **16**, 2446-2460, (2008)
- [25]. R. Amin, J. Zhou, A. Gilerson, B. Gross, F. Moshary, and S. Ahmed, "Novel optical techniques for detecting and classifying toxic dinoflagellate *Karenia brevis* blooms using satellite imagery," *Opt. Express* **17**, 9126-9144, (2009)
- [26]. <http://oceancolor.gsfc.nasa.gov>
- [27]. H. R. Gordon, and M. Wang, "Retrieval of water-leaving radiance and aerosol optical thickness over the oceans with SeaWiFS: a preliminary algorithm," *Appl. Opt.* **33**, 443-452 (1994)
- [28]. Z. P. Lee, http://www.ioccg.org/groups/OCAG_data.html
- [29]. FWRI, <http://www.floridamarine.org>
- [30]. http://coastwatch.noaa.gov/hab/bulletins_ns.htm
- [31]. MacKee, A. Cunningham, D. Wright, and L. Hay, "Potential impacts of nonalgal materials on water-leaving Sun induced chlorophyll fluorescence signals in coastal waters," *Appl. Opt.* **46**, 7720-7729, (2007)
- [32]. M. C. Tomlinson, T. T. Wynne, and R. P. Stumpf, "An evaluation of remote sensing techniques for enhanced detection of the toxic dinoflagellate, *Karenia brevis*," *Remote Sens. Environ.*, doi:10.1016/j.rse.2008.11.003, (2008)
- [33]. Hu, Z. P. Lee, F. E. Muller-Karger, and K. L. Carder, "Application of an optimization algorithm to satellite ocean color imagery: A case study in Southwest Florida coastal waters," In J. Frouin, Y. Yuan, & H. Kawamura (Eds.) *SPIE Proceedings. Ocean Remote Sensing and Applications*, vol. 4892 (pp. 70-79). Bellingham, WA: SPIE, (2003)
- [34]. http://research.myfwc.com/features/category_sub.asp?id=5301
- [35]. http://ocean.floridamarine.org/mrgis_ims/Description_Layers_Marine.htm#hab
- [36]. L. Young, M. Christman, "Team Analyzes Data To Answer Important Natural Resources Question", 2006 Annual Research Report: Florida Agricultural Experiment Station, p. 24--25
- [37]. <ftp://oceans.gsfc.nasa.gov/MODISA/Mapped/Daily/4/>
- [38]. R. Duda, P. Hart, D. Stork, "pattern Classification", Second Edition, Wiley-Interscience.